IOP PUBLISHING JOURNAL OF PHYSICS D: APPLIED PHYSICS

J. Phys. D: Appl. Phys. **45** (2012) 305303 (5pp) doi:10.1088/0022-3727/45/30/305303

Stress-induced annihilation of Stone–Wales defects in graphene nanoribbons

Y J Sun[1], F Ma[1,4], D Y Ma[1], K W Xu[1,2,4] and Paul K Chu[3]

[1] State Key Laboratory for Mechanical Behavior of Materials, Xi'an Jiaotong University, Xi'an 710049, Shaanxi, People's Republic of China

[2] Department of Physics and Opt-electronic Engineering, Xi'an University of Arts and Science, Xi'an 710065, Shaanxi, People's Republic of China

[3] Department of Physics and Materials Science, City University of Hong Kong, Tat Chee Avenue, Kowloon, Hong Kong, People's Republic of China

E-mail: mafei@mail.xjtu.edu.cn and kwxu@mail.xjtu.edu.cn

Received 25 April 2012, in final form 21 June 2012
Published 13 July 2012
Online at stacks.iop.org/JPhysD/45/305303

Abstract

Stress arising from structural or thermal misfit impacts the reliability of graphene-related devices. The deformation behaviour of graphene nanoribbons (GNRs) with Stone–Wales defects under stress studied by molecular dynamics shows that nearly all the SW defects annihilate *via* inverse rotation of C–C bonds. The fracture stress of defective GNRs is comparable to that of perfect ones and similar to mechanical annealing observed from bulk metals. It is a competition between bond rotation and fracture and depends on the strain rate and temperature. At a lower strain rate, such as 10^{-5} ps^{-1}, the rotation velocity of C–C bonds of 4.2 Å ps^{-1} is three orders of magnitude larger than the velocity of the collective movement of atoms (1.2×10^{-3} Å ps^{-1}). There is enough time for the C–C bond rotation to respond to the external load, but it becomes more difficult at higher strain rates. This stress-induced SW defect annihilation can be enhanced at higher temperatures because of enhanced exchange of atomic momentum and energy. The results reveal the dominant influence of SW defects on the mechanical properties of two-dimensional materials.

(Some figures may appear in colour only in the online journal)

1. Introduction

Graphene possesses outstanding physical properties, such as higher electron mobility [1], higher thermal conductivity [2, 3] and excellent mechanical strength [4], and is a potential candidate to replace silicon in next-generation microelectronics. In practical applications, the ultra-thin two-dimensional (2D) materials, with a thickness of only one monolayer, should be attached to some heterogeneous substrates. The structural and thermal misfit may induce stress, which can compromise the reliability and stability of the devices [5, 6]. Hence, the mechanical behaviour of graphene is crucial and although much experimental and theoretical work is being conducted, most of it focuses on perfect crystals. However, defects are ubiquitous in graphene fabricated by chemical vapour deposition (CVD) [7, 8] or thermal decomposition of 6H-SiC [9, 10]. The typical ones are Stone–Wales (SW) topological defects which are pairs of five- and seven-membered carbon rings formed by the rotation of C–C bonds by 90°. Grain boundaries, which can be considered to be an array of SW defects, have been observed by annular dark-field scanning transmission electron microscopy [11]. The effects of these defects on the mechanical behaviour of graphene are still not well understood. It is generally agreed that the mechanical behaviour and strength of bulk metals are dominated by the multiplication, movement, as well as annihilation of dislocations. Since SW defects resemble dislocations in topology, they are expected to be crucial to the deformation of this 2D system.

Based on molecular dynamics simulation of the in-plane tensile loading process, Grantab *et al* [12] found that graphene with large-angle tilt boundaries is as strong as the pristine

[4] Authors to whom any correspondence should be addressed.

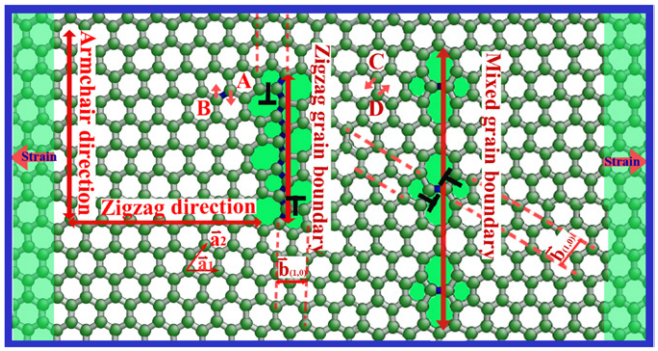

Figure 1. Schematic model of SW topological defects and grain boundary in graphene.

one and unexpectedly much stronger than that with low-angle boundaries. In general, the large-angle boundaries are stronger because they can better accommodate the strained rings through in-plane bond rotation. Huang *et al* [11] fabricated single-layer graphene on copper foils by CVD and evaluated the mechanical strength by AFM indentation. It was demonstrated that the graphene broke along the large-angle grain boundaries at loads of ∼100 nN, which was an order of magnitude lower than the typical fracture loads of 1.7 μN for single-crystal exfoliated graphene. The results appear to be inconsistent with Grantab's model. On the one hand, the loading mode is different. The loading in the model is along the in-plane direction, whereas the loading in the experiment is along the out-of-plane direction in which the activation of in-plane bond rotation is difficult. On the other hand, the loading strain rate used in the simulation is several orders of magnitude larger than that adopted in the AFM indentation process. If the different mechanical properties are indeed caused by the difference in the loading mode as well as loading conditions, it is critical to clarify the dominant effects of these factors on the evolution of SW defects under stress.

In this work, the in-plane deformation behaviour of graphene nanoribbons (GNRs) with SW defect arrays by atomic-scale simulation is studied. We mainly focus on the evolution of the SW defects under stress as well as the dependence on the strain rate and temperature. The mechanical properties of this 2D system are determined in order to gain an insight into the device design.

2. Simulation model

The simulation model of zigzag graphene nanoribbons (ZGNRs) 150 × 150 Å in feature size is built up with 8540 atoms. The SW defects are introduced by 90° rotation of C–C bonds [13] and there are usually two types of SW defect arrangements, as schematically indicated in figure 1. In the first case, the SW defect is formed by the clockwise rotation of A–B bonds by 90°. A grain boundary will appear if a series of such C–C bond rotations takes place transforming the original crystalline direction from armchair into zigzag by inserting two perpendicular wedges up and down. The Burgers vector $\vec{b}$ can be expressed as $\vec{b} = n\vec{a}_1 + m\vec{a}_2 = n\vec{a}_1$, where $\vec{a}_{1,2} = (3d/2 \pm \sqrt{3}d/2)$ is the nearest neighbour interatomic distance and $d = 1.42$. The period of SW defects distributed along a grain boundary is $2.5d = 3.57$ Å. In the second case, the SW defects are formed by counter-clockwise rotation of C–D bonds. The lattice Burgers vector $\vec{b} = m\vec{a}_2$ and the period along the grain boundary is $5d = 7.13$ Å that is two times larger than that of the former case. It is equal to inserting two inclined wedges as indicated by the red dotted lines. In both cases, the grain boundaries are perpendicular to the edges of graphene ribbons. In order to guarantee the same ribbon width in these two systems, they consist of 13 and 6 pairs of SW defects, respectively, along the grain boundaries. A uniaxial stress is applied onto the side atoms indicated by the semitransparent green colour along the zigzag direction.

In the MD simulation implemented in the software package LAMMPS [14], the interaction between carbon atoms is described by the adaptive intermolecular reactive bond order (AIREBO) potential, which can accurately capture the interactions between carbon atoms as well as bond breaking and re-forming [15, 16]. The cutoff parameter describing the short-ranged C–C interactions is chosen to be 2.0 Å in order to avoid spuriously high bond forces and nonphysical results at large deformation [17, 18]. Before dynamics simulation, all the graphene sheets with periodic conditions in the two in-plane directions are relaxed to an equilibrium state in the isothermal–isobaric (NPT) ensembles at a certain temperature for 600 000 MD steps with a time step of 1 fs. GNRs are then created by deleting atoms outside the nanoribbons, and a vacuum region with 15 Å in width is added perpendicular to the zigzag direction so that the atoms near one edge of the GNRs do not interact with those near the opposite edge. The MD simulation of uniaxial tensile stress loaded along the zigzag direction is performed in the canonical (NVT) ensemble using a deformation-control method. Five strain rates ($\dot{\varepsilon}$) of 10^{-1}, 10^{-2}, 10^{-3}, 10^{-4} and 10^{-5} ps^{-1} are used. Temperature in the range from 1000 to 2500 K is applied using the Nose–Hoover thermostat, and the fracture stress and strain are calculated according to [19]. The layer separation of graphite, 3.4 Å, is taken as the effective thickness of the graphene monolayer [19] and Poisson's ratio is chosen to be 0.165 [20].

3. Results and discussion

The stress–strain curves of the graphene nanoribbons with defects (DGNRs) are similar to those previously observed from perfect ZGNRs. That is, the stress changes linearly with strain initially and then non-linear elasticity begins. Finally, the stress is reduced sharply at a certain strain corresponding to fracture (figure 2(*a*)). Figure 2(*b*) displays the fracture stress as a function of strain rates at typical temperatures of 1000, 1500, 2000 and 2500 K. The results of perfect ZGNRs are also shown for comparison. Obviously, the fracture stress increases with increasing strain rates but decreases with increasing temperature for both ZGNRs and DGNRs. The maximum fracture stress of ZGNRs is about 140 GPa at 1000 K and a strain rate of 10^{-1} ps^{-1} and it is consistent with the previously obtained values of 130 ± 10 GPa [4, 19]. The fracture stress is hardly affected due to the existence of SW defects, particularly at a lower strain rate and a higher temperature.

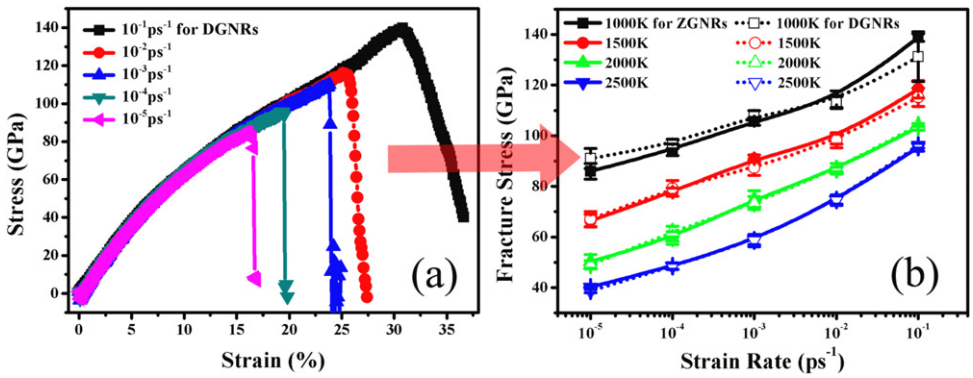

Figure 2. (*a*) Stress–strain curves of typical DGNRs at 1000 K and (*b*) fracture stress as a function of strain rate and temperature. The values are averages of five data points at each strain rate with error bars.

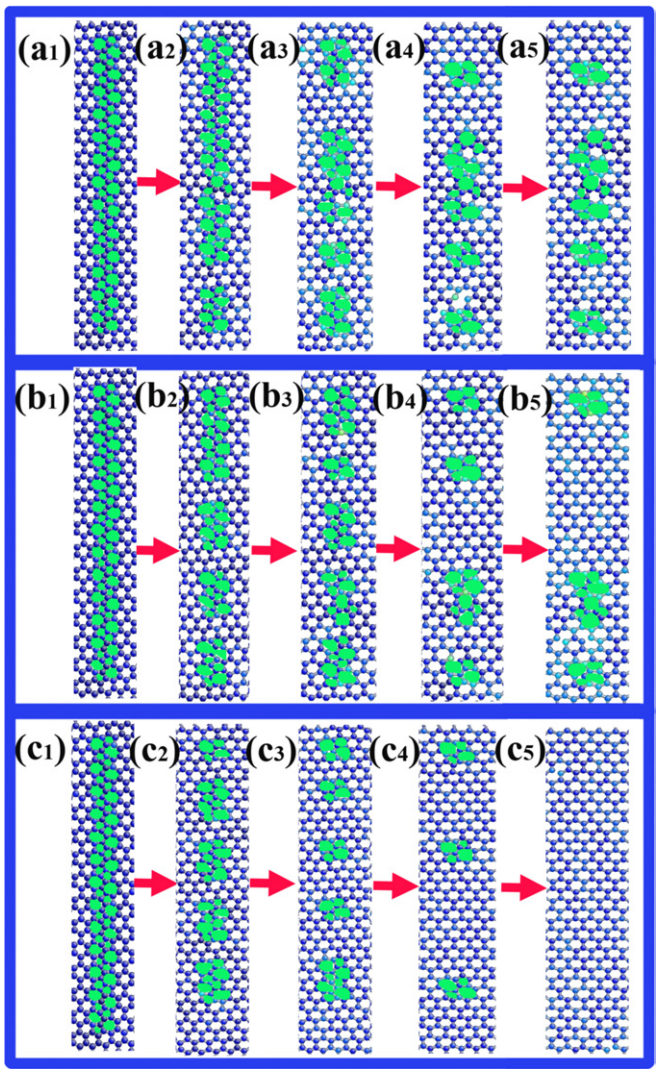

Figure 3. Atomic structure evolution of DGNRs as a function of tensile strain at strain rates of (*a*) 10^{-2} ps^{-1}, (*b*) 10^{-3} ps^{-1} and (*c*) 10^{-4} ps^{-1} at 1000 K. The tensile strain for 1, 2, 3, 4 and 5 panels is 0%, 5%, 10%, 15% and 20%.

Figure 3 presents the evolution of the atomic structure near the grain boundaries. Generally, some SW defects annihilate via inverse C–C bond rotation under an applied stress and the grain boundaries become segmented by perfect hexagons (figure 3). The annihilation number of SW defects increases gradually with strain and depends on the strain rate and temperature sensitively. The lower the strain rate (figure 4(*a*)) and the higher the temperature (figure 4(*b*)), the more quickly defect annihilation takes place. The influence of temperature is more significant and there is a competition between bond rotation and bond fracture. For a given GNR with length L_0, the velocity of the collective movement of atoms at a strain rate of $\dot{\varepsilon}$ can be expressed as $V_0 = L_0 \cdot \dot{\varepsilon}$. The linear velocity corresponding to C–C bond rotation, V_1, can be calculated as $V_1 = L_1/\delta t$ in which L_1 is the displacement of carbon atoms accompanying bond rotation and is set as the bond length, 1.426 Å. δt is the annihilation time (0.34 ps) of SW defects obtained according to the state transition theory (TST) [21]. For the strain rate of $\dot{\varepsilon} = 10^{-2}\,\text{ps}^{-1}$, we have $V_1 = 4.2\,\text{Å ps}^{-1}$ and $V_0 = 1.2\,\text{Å ps}^{-1}$. If the strain rate is reduced to $10^{-3}\,\text{ps}^{-1}$, $V_0 = 0.12\,\text{Å ps}^{-1}$, which is one order of magnitude smaller than the velocity of bond rotation. Hence, the atoms have enough time to rotate and relax to the equilibrium state and so defect annihilation can take place kinetically and will be improved if the strain rate is reduced further. At a strain rate of $10^{-4}\,\text{ps}^{-1}$, almost all the defects disappear at a strain of 20% leading to perfect GNRs (figure 3(*c*5)). Therefore, it is not difficult to image that fracture should take place at the same stress for ZGNRs and DGNRs. This also demonstrates the dominant effect of the bond rotation defects on the mechanical behaviour of graphene, as observed in a previous MD simulation [12]. The stress-induced annihilation of SW defects can be treated as mechanical annealing similar to the dislocation behaviour in metals and alloys [22]. This annihilation process is accelerated at higher temperatures because of the enhanced exchange of atomic momentum and energy (figure 4(*b*)). However, annihilation of SW defects will be suppressed at a temperature below 1000 K.

Figure 5(*a*) shows the potential energy of DGNRs under tensile loading at a strain rate of $10^{-3}\,\text{ps}^{-1}$ at 1000 K. As indicated by the bold blue line, the average potential energy of the entire DGNRs increases gradually from −7.30 eV (at an equilibrium state, consistent with the value of −7.39 eV for the planar pristine graphene monolayer [23]) with increasing strain. The average potential energy per atom near SW defects (E_0), as indicated by the thin green line, also increases with

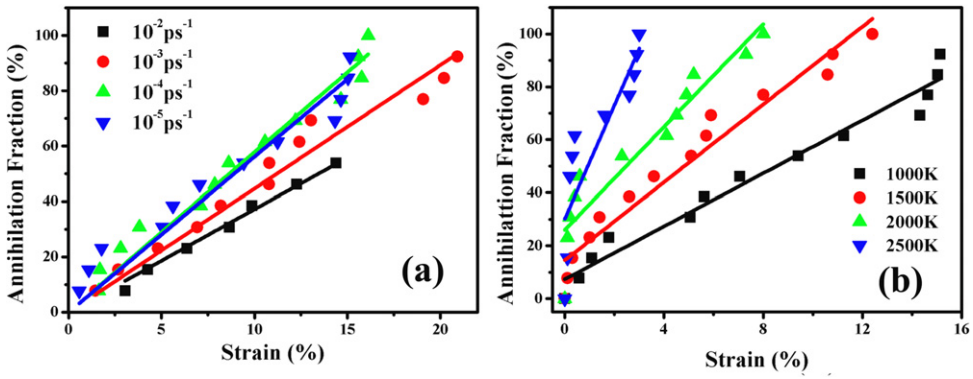

Figure 4. (*a*) Annihilation fraction of SW defects as a function of strain for different strain rates at 1000 K and (*b*) for different temperatures at a strain rate of 10^{-4} ps^{-1}.

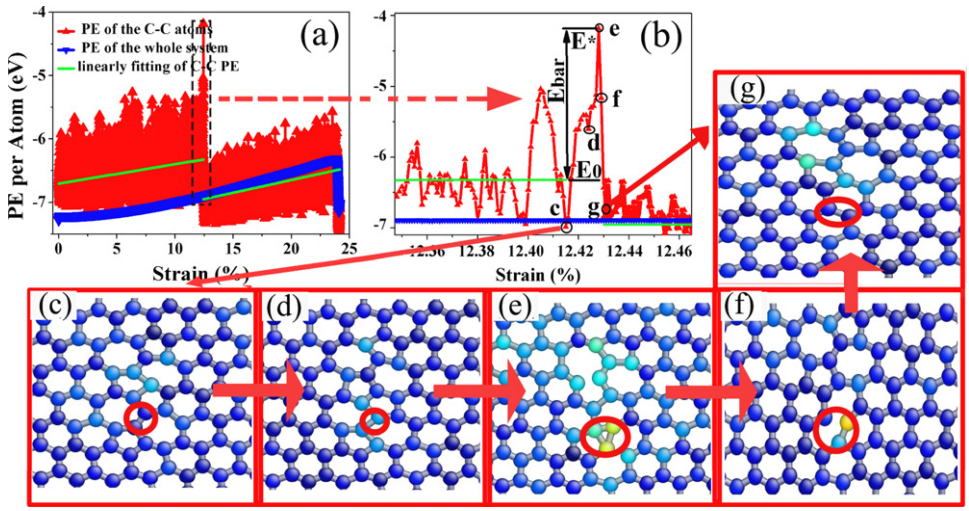

Figure 5. Variation of potential energy per atom (*a*) and (*b*) and atomic structure evolution (*c*)–(*g*) of SW defects at 1000 K and strain rate of 10^{-3} ps^{-1}. In (*a*), the red dotted line presents the potential energy of SW defects, the green line indicates the average value and the blue line is the average of the whole system. The magnification of the region in which the potential energy changes sharply is displayed in (*b*). E_0 is the average potential energy fitted from the green line, E^* is the maximum potential energy of atoms in the SW defects and $E_{\rm bar}$ is the energy barrier for the annihilation of SW defects.

strain, but is 0.5 eV higher than that of the whole system. When the tensile strain is increased to 12.4%, the averaged potential energy, E_0, increases to a peak value of about −4.1 eV (E^*) and then decreases sharply to the average value of the whole DGNRs (figures 5(*a*) and (*b*)). In fact, this process corresponds to annihilation of SW defects as a result of inverse rotation of C–C bonds. The energy barrier can be calculated as $E_{\rm bar} = E^* - E_0$ and is about 1.9 eV. The detailed structure evolution is illustrated in figures 5(*c*)–(*g*). The potential energy per atom of the C–C bond denoted by a red circle at the centre of an SW defect has the lowest value at the atomic configuration of figure 5(*c*) and increases gradually accompanied by increased bond lengths from 1.39 to 1.70 Å (figure 5(*d*)). As the strain is further increased, a triangle transition structure (figure 5(*e*)) appears as a result of C–C bond rotation by 45°. The potential energy peak is reached and meanwhile, the upper SW defect disappears. Afterwards, one bond of this triangular structure ruptures to form the hexagonal lattice and promotes annihilation of the SW defects (figures 5(*f*) and (*g*)). The potential energy is significantly reduced to the level of the whole GNRs (figure 5(*b*)). This two-step process can considerably reduce the energy barrier required for the annihilation of SW defects. It is equal to the reverse process of SW defect formation [24]. However, the energy barrier obtained is two or three times less than that required for defect formation and it may be due to the mechanical stress-induced transition triangular structure. This stress-induced annihilation of SW defects is not found in the case of a mixed grain boundary (right-hand side of figure 1) even at the lowest strain rate of 10^{-5} ps^{-1}, as shown in figure 6. In fact, rotation of the bonds at the centre of the SW defects is required for annihilation. Unfortunately, in the mixed grain boundary, these bonds are parallel to the applied stress and so there is no effective moment of force. Consequently, it is difficult for the bonds to rotate to annihilate the SW defects. Although the SW topological defects in graphene resemble the dislocations in three-dimensional (3D) metals, their annihilation mechanisms are absolutely different from each other. For the dislocations in 3D metals, they annihilate through slipping out of the surface, and thus the smaller the material size, the easier the dislocations disappear. But for the SW topological defects in graphene, they annihilate through

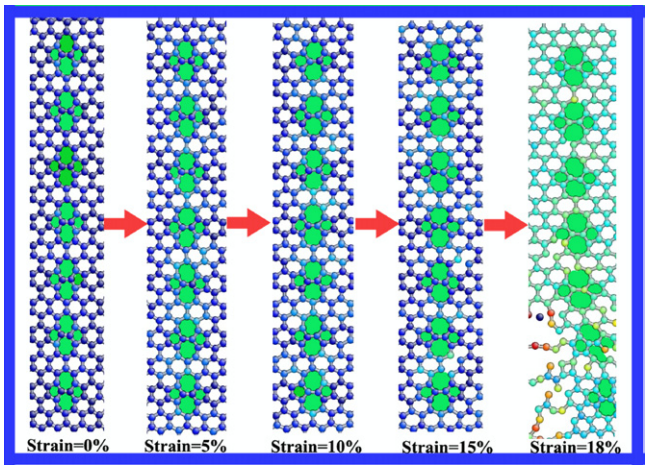

Figure 6. Atomic structure evolution of DGNRs with a mixed grain boundary as shown on the right-hand side of figure 1 at a strain rate of 10^{-5} ps^{-1}.

the rotation of local C–C bonds instead of slipping and depend only on the potential energy barrier in the bond rotation. It is environment sensitive but not size dependent. It may be one of the differences between 3D and 2D materials.

4. Conclusions

Graphene, which possesses excellent electronic properties, should be attached to some heterogeneous substrates in applications. There are structural and thermal misfits between the graphene and substrates. They usually induce considerable stress and undermine the reliability of devices. The deformation behaviour of graphene with SW defects under stress is studied by MD simulation. The fracture stress increases with strain rates but decreases with increasing temperature. Unexpectedly, the fracture stress of defective graphene is almost the same as that of the perfect one because nearly all SW defects can be annihilated via inverse C–C bond rotation under mechanical loading. The stress-induced defect annihilation depends on the strain rate and temperature. At a lower strain rate, the velocity of atoms due to external loading is several orders of magnitude smaller than that of the velocity corresponding to C–C bond rotation. Hence, defect annihilation is activated. If the strain rate is increased, bond rotation cannot respond to the external deformation in time. This annihilation process can be enhanced at a higher temperature because of accelerated exchange of atomic momentum and energy. Our results suggest that the mechanical properties of monolayered graphene are extremely sensitive to the loading conditions and environment.

Acknowledgments

This work was jointly supported by the Key Project of the Chinese National Programs for Fundamental Research and Development (Grant No 2010CB631002), the National Natural Science Foundation of China (Grant No 50901057, 51171145), National Ministries and Commissions (Grant No 6139802-04), New Century Excellent Talents in University, Fundamental Research Funds for the Central Universities and Hong Kong Research Grants Council (RGC) General Research Funds (GRF) No CityU 112510.

References

[1] Novoselov K S, Geim A K and Morozov S V 2004 *Science* **306** 666
[2] Alexander A B, Suchismita G, Bao W Z and Irene C 2008 *Nano Lett.* **8** 902
[3] Jae H S, Insun J, Arden L M, Lucas L, Zachary H A and Michael T P 2010 *Science* **328** 9
[4] Lee C G, Wei X D, Jeffrey W K and James H 2008 *Science* **321** 18
[5] Ferralis N, Maboudian R and Carraro C 2008 *Phys. Rev. Lett.* **101** 156801
[6] N'Diaye A T, Gastel R V, Martínez-Galera A J and Coraux J 2009 *New. J. Phys.* **11** 113056
[7] Haider I R, Emil B S, Matthew J A and Jonathan K W 2011 *Nano Lett.* **11** 251
[8] Li X S, Carl W M, Archana V and Jinho A 2010 *Nano Lett.* **10** 4328
[9] Glenn G J, Brenda L V, Joseph L T and Joseph G T 2009 *Nano Lett.* **9** 2605
[10] Rutter G M, Crain J N, Guisinger N P, Li T, First P N and Stroscio J A 2007 *Science* **317** 219
[11] Huang P Y, Ruiz-Vargas C S, Zande A M and Whitney W S 2011 *Nature* **469** 389
[12] Grantab R, Vivek B S and Rodney S R 2010 *Science* **330** 946
[13] Oleg V Y and Steven G L 2010 *Phys. Rev.* B **81** 195420
[14] Plimpton S 1995 *J. Comput. Phys.* **117** 1
[15] Stuart S J, Tutein A B and Harrison J A 2000 *J. Chem. Phys.* **112** 6472
[16] Brenner D W, Shenderova O A, Harrison J A and Stuart S J 2002 *J. Phys. Condens. Matter* **14** 783
[17] Pei Q X, Zhang Y W and Shenoy V B 2010 *Carbon* **48** 898
[18] Shenderova O A and Brenner D W 2000 *Phys. Rev.* B **61** 3877
[19] Zhao H, Min K and Aluru N R 2009 *Nano Lett.* **9** 3012
[20] Zhou J and Huang R J 2008 *J. Mech. Phys. Solids.* **56** 1609
[21] Peter H, Peter T and Michal B 1990 *Rev. Mod. Phys.* **62** 2
[22] Shan Z W, Mishra R K, Asif S A S, Warren O L and Minor A M 2008 *Nature Mater.* **7** 115
[23] Lu Q and Huang R 2010 *Phys. Rev.* B **81** 155410
[24] Li L, Reich S and Robertson J 2005 *Phys. Rev.* B **72** 184109